

## “Superlattices” in quenched Al-Si-Mn quasicrystals

C. H. Chen and H. S. Chen

*AT&T Bell Laboratories, Murray Hill, New Jersey 07974*

(Received 18 November 1985)

Melt-quenched  $\text{Al}_{74}\text{Si}_6\text{Mn}_{20}$  and  $\text{Al}_{72}\text{Si}_6\text{Mn}_{22}$  alloys were found to exhibit icosahedral symmetry with a “superlattice-like” diffraction pattern which can be reproduced from the pattern observed in  $\text{Al}_{86}\text{Mn}_{14}$  quasicrystals with a scaling relationship defined by the golden mean.

An alloy of Al with 14 at. % Mn formed by rapid quenching was recently found to have a long-range orientational order with an electron diffraction pattern consistent with icosahedral point group symmetry.<sup>1</sup> The appearance of sharp diffraction spots can be explained by a new class of ordered structures (quasicrystals) with quasiperiodic rather than periodic translational order.<sup>2</sup> Calculated diffraction intensity patterns<sup>2</sup> for an ideal icosahedral quasicrystal agree remarkably well with the experimental results observed in the quenched Al-Mn samples. Other phenomenological models based upon Landau theory with quasiperiodic translational order and icosahedral point symmetry have also been proposed.<sup>3–6</sup> Using an icosahedral reciprocal lattice, all the peaks observed in the electron and x-ray diffraction of quenched  $\text{Al}_{86}\text{Mn}_{14}$  can be indexed with a quasilattice parameter.<sup>7,8</sup> In this paper, we report electron diffraction studies of quenched  $\text{Al}_{74}\text{Si}_6\text{Mn}_{20}$  and  $\text{Al}_{72}\text{Si}_6\text{Mn}_{22}$  alloys. The diffraction patterns observed in these alloys can be closely reproduced from the patterns observed in  $\text{Al}_{86}\text{Mn}_{14}$  quasicrystal by a scaling relationship defined by the golden mean,  $\tau = (\sqrt{5} + 1)/2$ . This is the first time a “superlattice-like” diffraction pattern has been observed in systems with icosahedral symmetry.

Al-Si-Mn alloys were made by induction melting of high purity Al, Si, and Mn in a boron-nitride crucible under argon atmosphere. Ribbons of about 1 mm in width and 30  $\mu\text{m}$  in thickness were obtained by melt spinning in an argon atmosphere. Samples for transmission electron microscopy (TEM) were prepared by chemical thinning in an acid solution containing  $\text{H}_3\text{PO}_4$ ,  $\text{H}_2\text{SO}_4$ , and  $\text{HNO}_3$  at 75°C. The specific heat and kinetics of transformation were measured with a Perkin-Elmer DSC-2 calorimeter. It was found that partial substitution of Al by 6 at. % of Si considerably stabilizes the icosahedral phase. The main transition region between 680 and 780 K observed in  $\text{Al}_{86}\text{Mn}_{14}$  (Ref. 9) has moved up to a much higher-temperature range  $\sim 820$ – $920$  K. However, the heat of transformation is  $\sim 560$  cal/mol for  $\text{Al}_{74}\text{Si}_6\text{Mn}_{20}$ , which is identical to that observed in  $\text{Al}_{86}\text{Mn}_{14}$ .

TEM examination of  $\text{Al}_{80}\text{Mn}_{20}$  quenched samples shows a mixture of the icosahedral phase and a phase which is known as “*T*” phase.<sup>10</sup> Details of this phase and the structures observed in samples with higher Mn content will be published elsewhere.<sup>11</sup> Electron diffraction patterns of the icosahedral phase are identical to those

found in the  $\text{Al}_{86}\text{Mn}_{14}$ . Partial substitution of Al with 6 at. % Si ( $\text{Al}_{74}\text{Si}_6\text{Mn}_{20}$ ) results in striking changes in the structure. First of all, the “*T*” phase disappears and only the icosahedral phase remains. Moreover, electron diffraction patterns from a single icosahedral domain reveal perfect icosahedral point symmetry just like those of  $\text{Al}_{86}\text{Mn}_{14}$ . However, in this case more diffraction spots can be seen in a given range of scattering angles in comparison with the diffraction patterns observed in the icosahedral  $\text{Al}_{86}\text{Mn}_{14}$  and  $\text{Al}_{80}\text{Mn}_{20}$ . Figures 1(b), 1(d), and 1(f) show selected-area electron diffraction patterns in  $\text{Al}_{74}\text{Si}_6\text{Mn}_{20}$  which exhibit five-, three-, and twofold symmetries, respectively. For comparison, the corresponding diffraction patterns observed in the icosahedral phase  $\text{Al}_{80}\text{Mn}_{20}$  are also shown in Figs. 1(a), 1(d), and 1(e), which are identical to the patterns observed in  $\text{Al}_{86}\text{Mn}_{14}$ .<sup>1,12</sup> Comparison of the five- and also the three-fold patterns are straightforward. If we examine the intensity distribution pattern of spots surrounding a series of chosen diffraction spots, it is apparent that Figs. 1(b) and 1(d) can be obtained by scaling down Figs. 1(a) and 1(c), respectively, by the golden mean. Hence the experimental results from the five- and three-fold patterns suggest that we have a quasicrystal “superlattice” in  $\text{Al}_{74}\text{Si}_6\text{Mn}_{20}$  with a quasilattice parameter greater by the golden mean than that observed in the icosahedral  $\text{Al}_{86}\text{Mn}_{14}$  and  $\text{Al}_{80}\text{Mn}_{20}$  quasicrystals. The relationship between the two-fold patterns shown in Figs. 1(e) and 1(f), however, is not as simple, although the appearance of superlattice [Fig. 1(f)] diffraction spots is quite obvious. Following the same guidelines of comparison mentioned above we find that a nonuniform scaling is required. Specifically, a scaling factor  $\tau$  along the *x* axis and a scaling factor  $\tau^2$  along the *y* axis can transform Fig. 1(e) into Fig. 1(f) without loss (or addition) of existing (or extra) visible diffraction spots. Two rhombuses are marked in Figs. 1(e) and 1(f) for ease of comparison. We note that Figs. 1(b), 1(d), and 1(f) cannot be obtained by simply adding extra spots in Figs. 1(a), 1(c), and 1(e) because the intensities of the corresponding spots would be different. The intensity profile of the diffraction spots along a symmetry direction in Al-Si-Mn would be very similar to the corresponding intensity profile in Al-Mn if the length scales in the reciprocal space are scaled by the golden mean relationship mentioned above. We, therefore, have an unusual kind of quasicrystal “superlattice” which cannot be described with a uniform scaling factor  $\tau$ . We note

that the diffraction spots in the "superlattice" phase appear sharper than the spots in the regular icosahedral phase. Whether the widths of spots of the two phases are scaled by the golden mean, cannot be determined accurately in our case.

TEM examination of  $\text{Al}_{74}\text{Si}_6\text{Mn}_{20}$  also reveals quite different morphology as compared to domain structures in binary alloys  $\text{Al}_{86}\text{Mn}_{14}$  and  $\text{Al}_{80}\text{Mn}_{20}$ . In  $\text{Al}_{86}\text{Mn}_{14}$  the icosahedral domains are characterized by the appearance of elongated branches stemming from a central nodule within the domain and also by fine ( $\sim 150 \text{ \AA}$ ) speckles in the domain. Domain boundaries are jagged due to the presence of the elongated branches. The dendritic growth found in  $\text{Al}_{86}\text{Mn}_{14}$  is absent in the icosahedral domains of  $\text{Al}_{80}\text{Mn}_{20}$ ; nevertheless, the domain boundaries in this case are still quite irregular in shape. In the case of  $\text{Al}_{74}\text{Si}_6\text{Mn}_{20}$  the domains have uniform contrast free of

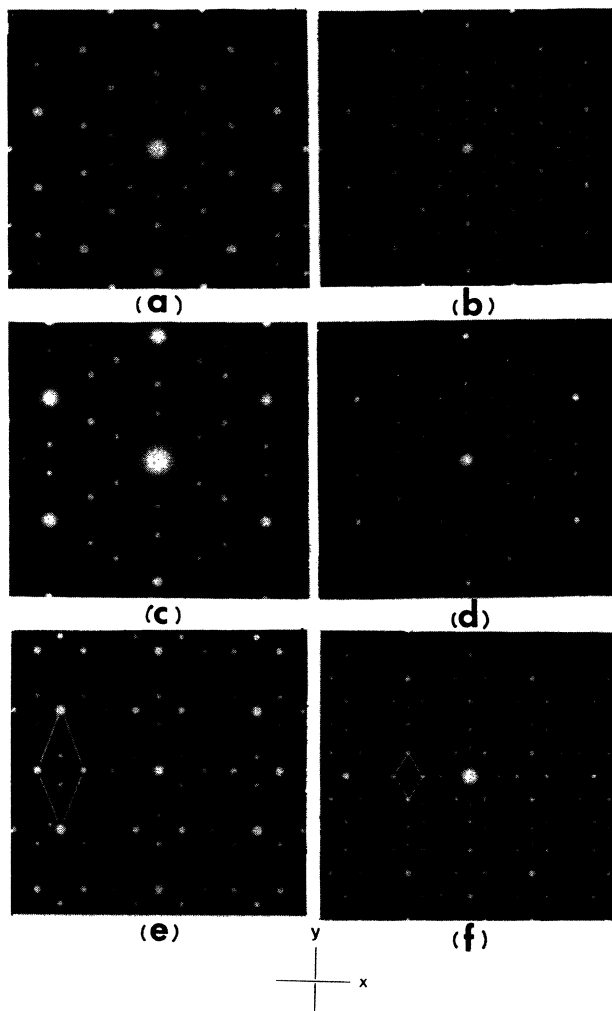


FIG. 1. (a), (c), and (e) are selected area electron diffraction patterns from the icosahedral phase of  $\text{Al}_{80}\text{Mn}_{20}$  showing five-, three-, and two-fold symmetries, identical to the patterns observed in  $\text{Al}_{86}\text{Mn}_{14}$ ; (b), (d), and (f) are diffraction patterns obtained from  $\text{Al}_{74}\text{Si}_6\text{Mn}_{20}$  superlattice quasicrystals, which exhibit five-, three-, and twofold symmetries. The two rhombuses marked in (e) and (f) are for ease of comparison.

elongated branches and the domain boundaries are faceted as in intermetallic crystalline materials (Fig. 2). The size of the superlattice domain is typically  $\lesssim 1 \mu\text{m}$  as in  $\text{Al}_{86}\text{Mn}_{14}$  and in the  $\text{Al}_{80}\text{Mn}_{20}$  icosahedral phase. All these observations indicated the dramatic enhancement of structural order and stability by partial substitution of Al with 6 at. % Si in  $\text{Al}_{80}\text{Mn}_{20}$  quenched alloys. Apparently, the change in local bonding with the addition of Si produces a much higher degree of order in the overall structure.

The effect of changing Si and Mn concentration on the formation of the superlattice was also studied. We first examined the quenched alloys of  $\text{Al}_{94-y}\text{Si}_6\text{Mn}_y$  with  $y=14, 16, 18, 22, 24,$  and  $26$ . The "superlattice" system just discussed above corresponds to the alloy of  $y=20$ . Our experimental findings can be summarized as follows: (1) No quasicrystal "superlattice" can be seen in the alloys of lower Mn concentrations with  $y=14, 16,$  and  $18$ . These alloys exhibit diffraction patterns characteristic of the regular icosahedral quasicrystal with large domains ( $\lesssim 1 \mu\text{m}$ ) except in the case of  $y=14$ , where icosahedral domains are down to a few hundred  $\text{\AA}$  in size. (2) The alloy with  $y=22$  produces exactly the same "superlattice" as that observed in the alloy of  $y=20$ . The morphology of the domains is also very similar. (3) Alloys of higher Mn concentrations with  $y=24$  and  $26$  do not form an icosahedral phase. In fact,  $y=24$  produces a single crystal diffraction pattern, whereas  $y=26$  yields a phase that is very similar to the "T" phase mentioned earlier. Next, we studied the quenched ternary alloys with a Mn concentration fixed at 20 at. % and varying Si concentration (i.e.,  $\text{Al}_{80-x}\text{Si}_x\text{Mn}_{20}$ ). We examined quenched alloys with  $x=3, 6, 13,$  and  $20$ . It was found that the alloy with  $x=3$  has a very strong tendency for the "superlattice" formation. The alloy with  $x=13$ , quite surprisingly, was found to exhibit very diffuse diffraction haloes characteristic of amorphous phases, whereas the alloy with  $x=20$  exhibits a mixture of icosahedral and single crystalline phases. A detailed analysis of these numerous experimental results will be published elsewhere. From these studies it appears that the quasicrystal "superlattice" exists only in a narrow composition range of Si and Mn.

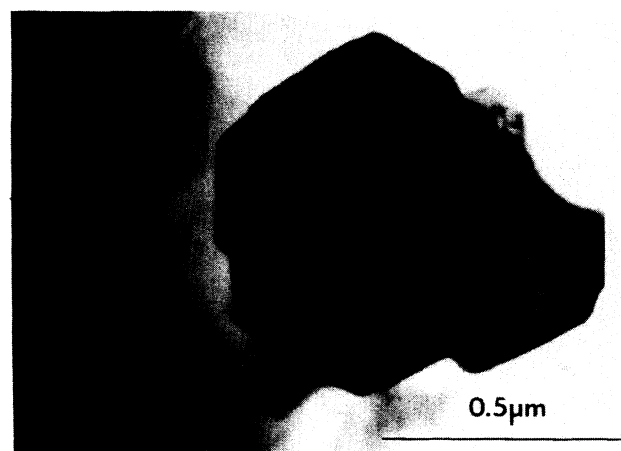


FIG. 2. Bright field electron micrograph showing the faceted superlattice domains in  $\text{Al}_{74}\text{Si}_6\text{Mn}_{20}$ .

The optimum compositions in  $\text{Al}_{100-x-y}\text{Si}_x\text{Mn}_y$  for the formation of "superlattice" seem to be  $x=6$ , and  $y=20$  or 22.

The question of why the "superlattices" in  $\text{Al}_{74}\text{Si}_6\text{Mn}_{20}$  and  $\text{Al}_{72}\text{Si}_6\text{Mn}_{22}$  quasicrystals can be scaled uniformly by  $\tau$  for the five- and three-fold patterns and not for the two-fold pattern is an interesting one. A two-fold icosahedral diffraction pattern is special in that diffraction spots with both even (scaled by  $\tau$ ) and odd (scaled by  $\tau^3$ ) parity sequences exist.<sup>7</sup> The physical significance of the  $\tau$ - $\tau^2$  scaling observed for the two-fold pattern in the superlattice phase is not clear at present. We know that the reciprocal lattice points of a quasicrystal are infinitely dense and indexing of the diffraction spots with a quasilattice constant can only be carried out by examining the intensity profile of a sequence of spots along a symmetry direction as a function of scattering angle. Under the projection scheme,<sup>7</sup> the intensity profile of a series of diffraction spots is determined by the  $q_{\perp}$ -dependent intensity function  $I(q_{\perp})$  in the so-called "pseudospace"—a space orthogonal to the experimental reciprocal space. The rapidly varying function  $I(q_{\perp})$ , which for convenience can be assumed to be Gaussian, is sensitively related to the structural order of an icosahedral lattice. Increasing the structural order has the effect of increasing the width of the Gaussian function  $I(q_{\perp})$  and therefore enhances the intensities of the diffraction spots at some given scattering angles. The most significant intensity enhancement should occur for those spots laying in the portion of  $I(q_{\perp})$  where  $I(q_{\perp})$  is changing rapidly; whereas little change is

expected for those weak spots laying in the tail of the Gaussian function  $I(q_{\perp})$ . It is evident that there are more weak diffraction spots visible in Fig. 1(f) than Fig. 1(e), which were taken under similar experimental conditions. Whether the "superlattice" phase can be interpreted in this way is not entirely clear. Of course, there are other theoretical factors that might improve the above simple picture deduced from the projection method and we shall have to await further theoretical developments in this area to fully understand our experimental results.

We mentioned earlier that the superlattice phase was structurally more stable than the icosahedral  $\text{Al}_{86}\text{Mn}_{14}$  phase. Vacuum annealing of  $\text{Al}_{86}\text{Mn}_{14}$  inside an electron microscope showed that the icosahedral phase transformed completely into the crystalline orthorhombic phase around 700 K. The "superlattice" phase of  $\text{Al}_{72}\text{Si}_6\text{Mn}_{22}$  remained stable up to  $\sim 750$  K. Above this temperature, a crystalline phase with a structure yet to be identified started to grow. However, even after heating at 850 K for 10 min, a mixture of the "superlattice" icosahedral phase and the crystalline phase is still obtained. The effect of a few at. % Si in Al-Mn alloys is quite remarkable, indeed. Recent NMR studies<sup>13</sup> of Al-Si-Mn alloy suggest a very different surrounding of the Al site in comparison with the Al-Mn quasicrystal. This fact may lead to the higher degree of order seen here.

We would like to thank V. Elser and D. R. Nelson for many valuable discussions.

<sup>1</sup>D. Shechtman, I. Blech, D. Gratias, and J. W. Cahn, *Phys. Rev. Lett.* **53**, 1951 (1984).

<sup>2</sup>D. Levine and P. J. Steinhardt, *Phys. Rev. Lett.* **53**, 2477 (1984).

<sup>3</sup>D. R. Nelson and S. Sachdev, *Phys. Rev. B* **32**, 689 (1985).

<sup>4</sup>N. D. Merriman and S. M. Troian, *Phys. Rev. Lett.* **53**, 1524 (1985).

<sup>5</sup>D. Levine, T. C. Lubensky, S. Ostlund, S. Ramaswamy, P. J. Steinhardt, and J. Toner, *Phys. Rev. Lett.* **54**, 1520 (1985).

<sup>6</sup>Per Bák, *Phys. Rev. Lett.* **54**, 1517 (1985).

<sup>7</sup>V. Elser, *Phys. Rev. B* **32**, 4892 (1985).

<sup>8</sup>P. A. Bancel, P. A. Heiney, P. W. Stephens, A. I. Goldman, and P. M. Horn, *Phys. Rev. Lett.* **54**, 2422 (1985).

<sup>9</sup>H. S. Chen, C. H. Chen, A. Inoue, and J. T. Krause, *Phys. Rev. B* **32**, 1940 (1985).

<sup>10</sup>D. Schechtman, R. J. Schaefer, and F. S. Blancaniello, *Metall. Trans.* **15A**, 1987 (1984).

<sup>11</sup>C. H. Chen and H. S. Chen (unpublished).

<sup>12</sup>K. F. Kelton and T. W. Wu, *Appl. Phys. Lett.* **46**, 1059 (1985).

<sup>13</sup>W. W. Warren, Jr., H. S. Chen, and J. J. Hauser, *Phys. Rev. B* **32**, 7614 (1985).

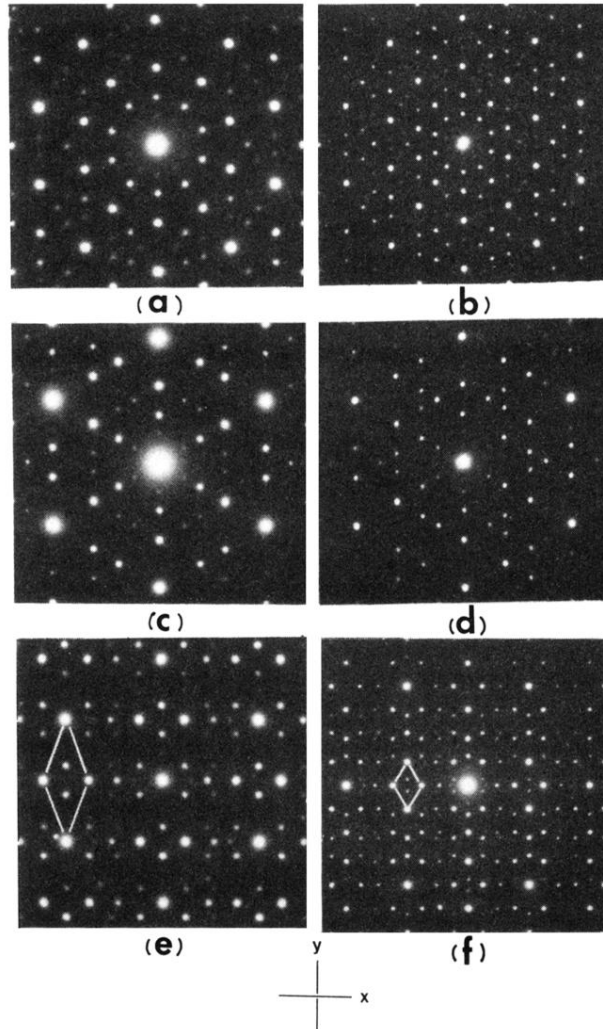


FIG. 1. (a), (c), and (e) are selected area electron diffraction patterns from the icosahedral phase of  $\text{Al}_{80}\text{Mn}_{20}$  showing five-, three-, and two-fold symmetries, identical to the patterns observed in  $\text{Al}_{86}\text{Mn}_{14}$ ; (b), (d), and (f) are diffraction patterns obtained from  $\text{Al}_{74}\text{Si}_6\text{Mn}_{20}$  superlattice quasicrystals, which exhibit five-, three-, and twofold symmetries. The two rhombuses marked in (e) and (f) are for ease of comparison.

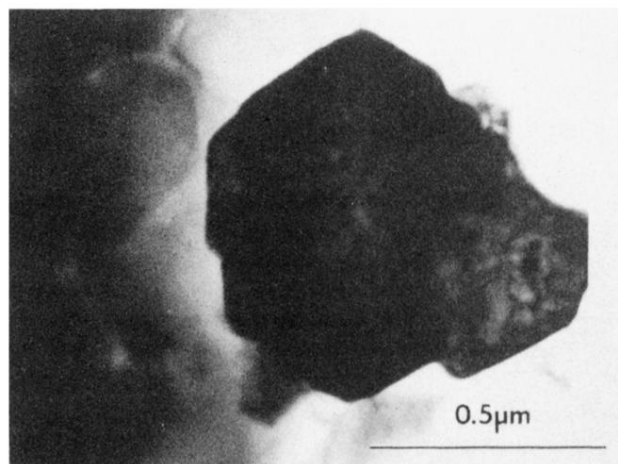


FIG. 2. Bright field electron micrograph showing the faceted superlattice domains in  $\text{Al}_{74}\text{Si}_6\text{Mn}_{20}$ .